Brownian Dynamics Close to a Wall Studied by Photon Correlation Spectroscopy from an Evanescent Wave

K. H. Lan,[a] N. Ostrowsky, and D. Sornette

Laboratoire de Physique de la Matière Condensée, Université de Nice, 06034 Nice Cèdex, France

(Received 27 December 1985)

Dynamic behavior of Brownian particles close to a wall is studied by photon correlation from an evanescent wave with variable penetration depth. Surface correlation spectra strongly differ from the bulk measurements and are completely interpreted in terms of the combined wall's mirror effect and evanescent-wave geometry. Relevance of these new effects to the light-scattering study of surface dynamics is discussed.

PACS numbers: 05.40.+j, 68.45.−v, 82.65.−i

In this Letter, we wish to report the first complete light-scattering study of the dynamics of free Brownian particles in the immediate proximity of a reflecting wall. The particles were probed by an evanescent wave[1] with variable penetration range, and the scattered light was analyzed at different angles with a photon-correlation technique.[2] It will be shown that the measured correlation spectrum, very different from the single exponential expected in the bulk geometry, may be simply and completely interpreted in terms of the combined wall's mirror effect and evanescent-wave geometry with no adjustable parameter. This effect is important and should be present in all experiments attempting to measure fluctuation dynamics at interfaces; it must therefore be accounted for and distinguished from other factors affecting the dynamics close to a surface, i.e., those due to the various wall-fluid interactions generally referred to as "surface effects."[3]

The evanescent-optical-wave technique is now well established in the field of polymer physics[4] and biophysics[5,6] for measuring various static properties, such as density profiles,[7] critical adsorption,[8] or surface adsorption kinetics,[9] and monitoring the fluorescence[10] from probes close enough to the wall to be excited by the evanescent field. One attempt to measure dynamic properties by the evanescent wave from an optical wave guide has been reported.[11] However, as the scattering particles were trapped in a multilamellar film parallel to the guide, only their lateral diffusion was measured and none of the new effects we have studied could be detected.

Our experimental setup is shown in Fig. 1. The fairly concentrated latex suspension (particle diameter $=0.09$ μm, $c \simeq 5\times10^{-4}$ g/cm^3, i.e., mean distance between particles $\simeq 1$ μm) is contained in a half cylindrical cell, sealed by the flat surface of a larger semicylinder glass prism. The sample holder is placed on a precision turntable, so as to easily change the incident angle θ_i of the vertically polarized He-Ne laser (30 mW at $\lambda_0 = 632.8$ nm). The critical angle θ_c of total reflection is given by the usual relation, $\sin\theta_c = n_L/n_G$, where $n_G = 1.48$ and $n_L = 1.33$ are the refraction index of the glass and the suspension, respectively. For $\theta_i > \theta_c$, the incident wave vector in the medium has a real component $k_i = 2\pi n_G \sin\theta_i/\lambda_0$, parallel to the flat surface of the prism, and an imaginary component equal to the inverse of the penetration depth ξ, given by[12]

$$\xi = (\lambda_0/2\pi n_G)[\sin^2\theta_i - \sin^2\theta_c]^{-1/2}. \quad (1)$$

The variation of ξ with θ_i was checked by monitoring the fluorescence intensity from a concentrated suspension of latex particles marked with rhodamine-B,[13] under the assumption that the density profile of the particles was uniform even close to the wall. This yielded for θ_c a value 64.3° close to the value 64.0° deduced from the above refraction indexes. The light scattered in the liquid at an angle θ from the incident wave vector $\mathbf{k}_i$ is collected through the glass prism (at an angle θ' such that $n_G\cos\theta' = n_L\cos\theta$) by a multimode fiber mounted on a rotating arm; photon correlation spectra were recorded in the range $30° \leq \theta \leq 110°$. Care was taken to align the optics in such a way that (i) a sufficient local-oscillator wave was mixed with the scattered light to ensure heterodyne detection, and (ii) the direction of the incident light

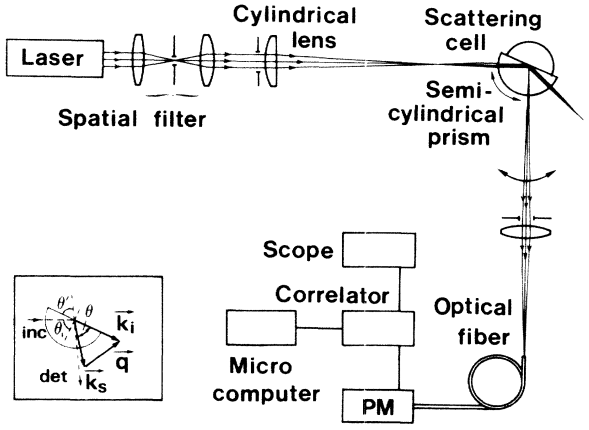

FIG. 1. Horizontal view of the experimental setup. Inset: Scattering geometry; $\mathbf{k}_i$ and $\mathbf{k}_s$ are, respectively, the incident and scattered wave vectors in the medium. The dashed lines show the incident and detection directions in the glass prism.

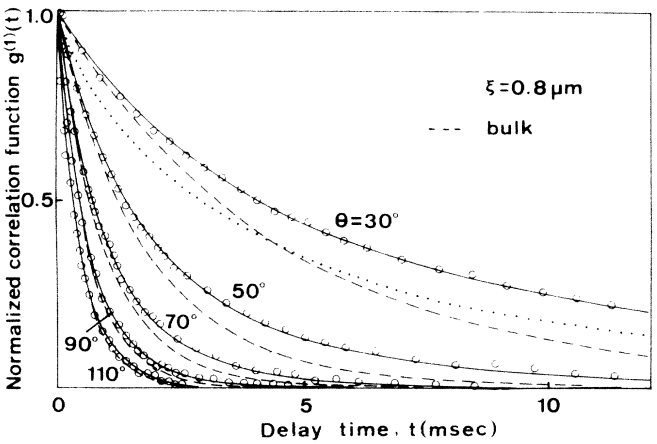

FIG. 2. Normalized autocorrelation spectra (circles) obtained at different scattering angles, for a fixed penetration depth. The dashed and solid lines are, respectively, the bulk and surface correlation functions. The dotted line shows a "bulk" correlation function (i.e., with the same illumination profile as the surface function but no wall).

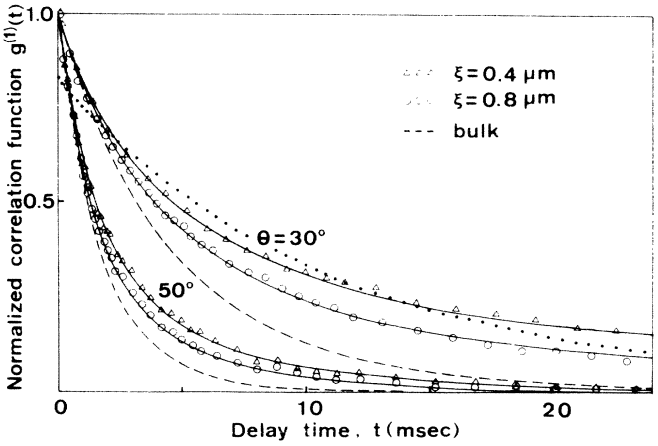

FIG. 3. Changes of the correlation spectra with the penetration depth. The dotted line shows the best single-exponential fit [yielding $D=(1.89\pm0.08)\times10^{-8}$ cm^2 s^{-1}] for a particular set of data ($\theta=30°$ and $\xi=0.4$ μm).

was tilted by a few degrees with respect to the horizontal plane. As a result, any partial back reflections on the cylindrical surface of the totally reflected laser light did not reenter the cell at the same height as the scattering volume; this eliminated any parasite "bulk" contribution to the scattered light.

Experimental correlation functions obtained at a fixed penetration depth ξ but for different scattering angles are shown in Fig. 2, together with the single-exponential decay expected in the bulk [see Eq. (4)]. In Fig. 3 are shown correlation functions at different penetration depths for two scattering angles. The smaller the scattering angle and the penetration depth, the more striking the difference between the experimental results and the usual "bulk" correlation function. The highly nonexponential behavior of the correlation function is emphasized in Fig. 3 where the best single-exponential fit for one set of data is shown with a dotted line.

To explain this new result, let us first recall that the signal measured in a heterodyne light-scattering experiment is the autocorrelation function $g^{(1)}(\mathbf{q},t)$ of the electric field scattered by a given particle,[2]

$$g^{(1)}(\mathbf{q},t)=\int\int_V \alpha^2 E_i(\mathbf{r})E_i(\mathbf{r}')\exp[i\mathbf{q}\cdot(\mathbf{r}'-\mathbf{r})]P(\mathbf{r},\mathbf{r}',t)\,d\mathbf{r}\,d\mathbf{r}', \tag{2}$$

where $E_i(\mathbf{r})$ and $E_i(\mathbf{r}')$ are the amplitudes of the incident electric fields at points $\mathbf{r}$ and $\mathbf{r}'$, and α is a constant related to the scattering angle and the polarizability of the particle as well as its size and shape. $P(\mathbf{r},\mathbf{r}',t)$ represents the usual probability density for a given particle to be at $\mathbf{r}$ at time zero and at $\mathbf{r}'$ at time t, and the integrals extend over the scattering volume V. The phase factor is determined by the scattering vector $\mathbf{q}=\mathbf{k}_i-\mathbf{k}_s$, where $\mathbf{k}_i$ and $\mathbf{k}_s$ are, respectively, the incident and scattered wave vectors in the liquid. Note that in the evanescent-wave geometry, $\mathbf{k}_i$ is always parallel to the flat surface of the prism, and its amplitude k_i only equals k_s (given by $2\pi n_L/\lambda_0$) for $\theta_i-\theta_c$. However, even for the smallest penetration depth $\xi=0.4$ μm, the incident angle was at most 2.2° away from θ_c and one can use the usual relation, $q=2k_i\sin\theta/2$, with an error less than 1%.

For an ensemble of free Brownian particles with diffusion constant D, the well-known expression[14]

$$P_B(\mathbf{r},\mathbf{r}',t)=(4\pi Dt)^{-3/2}\exp[-|\mathbf{r}-\mathbf{r}'|^2/4Dt] \tag{3}$$

yields, for a uniform illumination and isotropic particles, the usual single-exponential expression for the normalized correlation function in the bulk,[2]

$$g_B^{(1)}(\mathbf{q},t)=\exp(-Dq^2t), \tag{4}$$

which is shown with dashed lines in Figs. 2 and 3.

In the presence of a reflecting wall at $z=0$, the translation symmetry is broken and expression (3) must be replaced by[14]

$$P_s(\mathbf{r},\mathbf{r}',t)=(4\pi Dt)^{-3/2}\exp(-|\mathbf{r}_{\parallel}-\mathbf{r}'_{\parallel}|^2/4Dt)\{\exp[-(z-z')^2/4Dt]+\exp[-(z+z')^2/4Dt]\}, \tag{5}$$

where z and $\mathbf{r}_{\parallel}$ (z' and $\mathbf{r}'_{\parallel}$) are the components of $\mathbf{r}$ ($\mathbf{r}'$) normal and parallel to the wall. Obviously the mirror effect will come into play for times long enough for the distribution to reach the wall, but will be noticeable only if the distribution has not flattened out by then. If the presence of the wall was only to limit the volume available to the particle, its effect would be lost once the z integration in Eq. (2) is performed. The use of an evanescent wave,

however, enables us to limit this integration to values on the order of the penetration depth, ξ, small enough for this effect to be observed. Indeed, the incident electric fields $E_i(\mathbf{r})$ and $E_i(\mathbf{r}')$ appearing in (2) are no longer constant but decrease exponentially as $\exp(-z/\xi)$ and $\exp(-z'/\xi)$, respectively.

Using Eqs. (2) and (5) with these new profiles yields a surface correlation function of the form

$$g_s^{(1)}(\mathbf{q},t)=\exp(-Dq_{\parallel}^2 t)\,g_z(q_z,t), \tag{6}$$

where q_z and $\mathbf{q}_{\parallel}$ are the components of $\mathbf{q}$ normal and parallel to the wall. After a double integration from 0 to ∞ over z and z', $g_z(q_z,t)$ may be expressed in terms of the complementary error function:

$$g_z(q_z,t)=\mathrm{Re}[\exp(Z^2)\,\mathrm{erfc}(Z)]-(1/q_z\xi)\,\mathrm{Im}[\exp(Z^2)\,\mathrm{erfc}(Z)], \tag{7}$$

where $Z=[(Dt)^{1/2}/\xi](1+iq_z\xi)$ is a complex function of the two relevant dimensionless parameters, $(Dt)^{1/2}/\xi$ and $q_z\xi$. As long as $(Dt)^{1/2}/\xi$ is small compared to 1, the leading behavior of the correlation function is simply

$$g_s^{(1)}(\mathbf{q},t)=\exp(-Dq_{\parallel}^2 t)[1-Dt(1/\xi^2+q_z^2)]. \tag{8}$$

It decreases faster than $g_B^{(1)}(\mathbf{q},t)$ as $g_z(q_z,t)$ dies out not only if the scattering particle diffuses over a distance $1/q_z$, but also if it moves out of the scattering volume (i.e., if it diffuses over a distance ξ), the ratio of these two mechanisms being governed by the second parameter $q_z\xi$. This effect cannot be seen on our data since over the explored θ and ξ range, $q_z\xi$ remains in the interval (2.5,10).

In the other limit, $(Dt)^{1/2}/\xi \gg 1$, the surface correlation function can be expressed as

$$g_s^{(1)}(\mathbf{q},t)=\exp(-Dq_{\parallel}^2 t)[2/\sqrt{\pi}(1+q_z^2\xi^2)][\xi/(Dt)^{1/2}]. \tag{9}$$

This $t^{-1/2}$ long-time behavior is simply a finite-volume effect. The probability of still finding the initial particle in the scattering volume at time t decreases as $t^{-1/2}$. The smaller q_z^{ξ}, the larger this contribution is. Note that the long-time $t^{-1/2}$ evolution observed[15,16] for the number fluctuation function g_N has the same finite-volume origin; it must behave as $t^{-d/2}$, where d is the number of dimensions reduced to form the very thin scattering volume ($d=2$ in the usual cylindrical bulk geometry). In the evanescent-wave geometry, which has an intensity profile $\exp(-2z/\xi)$, we have worked out[17] the analytical expression for g_N:

$$g_N(t)=(1/\langle N\rangle)[(1-2X^2)\exp(X^2)\,\mathrm{erfc}(X)+2X/\sqrt{\pi}]\simeq(1/\langle N\rangle)[1/(\sqrt{\pi}X)], \quad \text{for } X\gg 1, \tag{10}$$

where $X=2(Dt)^{1/2}/\xi$ and $\langle N\rangle$ is the average number of particles in the scattering volume ($\simeq 10^4$ in our experiment). This signal, independent of the scattering angle, was, however, negligible in our heterodyne experiment.

To summarize the above discussion, we expect $g_z(q_z,t)$ to present large deviations from bulk behavior at intermediate or long time, provided q_z is small enough for the light to probe the medium over distances on the order of ξ.

Now, the measured correlation function $g_s^{(1)}(\mathbf{q},t)$ will provide information on its longitudinal component $g_z(q_z,t)$ only if the transverse factor $\exp(-Dq_{\parallel}^2 t)$ has a slow enough time dependence, i.e., $q_{\parallel} \lesssim q_z$. This explains why measurements at $\theta=\frac{1}{2}\pi\pm\alpha$, i.e., with the same q_z, exhibit different behavior. For example, in Fig. 2, measurements at $\theta=70°$ ($q_{\parallel}/q_z\simeq 0.7$) show a distinct deviation from the bulk correlation function, whereas for $\theta=110°$ ($q_{\parallel}/q_z\simeq 1.4$), the surface and bulk functions can no longer be distinguished.

The fits to the experimental data shown by solid lines on Figs. 2 and 3 were computed from Eqs. (6) and (7) with a seven-term expansion[18] for $\mathrm{erfc}(Z)$, consistent with the experimental noise ($\simeq 10^{-2}$). The penetration depth ξ was derived from Eq. (1), and the only adjustable parameter was the diffusion constant D, taking into account the sample polydispersity measured in the bulk ($Q\simeq 0.06$). All values found for D agreed with the value measured in the bulk to within 5% for $\xi=0.8$ μm and 8% for $\xi=0.4$ μm (see Table I), which proves the validity of Eq. (7) for a wide range of the parameters $(Dt)^{1/2}/\xi$ and $q_z\xi$. The remaining discrepancy, more pronounced for the smallest penetration depth, may have several origins, including a slowing down of the diffusion very close to the wall due to wall–fluid-particle drag effects,[19] possible partial adsorption, and the fact that the particle's radius R is not quite negligible compared to ξ.

Finally, to distinguish the wall's mirror effect from the finite-volume effect, we have shown with dotted lines on Fig. 2 the correlation function one expects with the same illumination profile, but in the abscence of the wall. It is obtained by omitting in Eq. (7) the term containing the imaginary part of $\exp(Z^2)\mathrm{erfc}(Z)$. This ficticious correlation function decays much faster at short times, as most of the scattering power comes from particles, initially at $z/\xi \ll 1$, which escape from the scattering volume by going to $z<0$. At long time, the $t^{-1/2}$ behavior is again observed, but with half the amplitude computed from Eq. (9) for the wall case; the mirror effect is responsible for this factor of 2.

To summarize, we have shown that the surface correlation function of free Brownian particles in the

TABLE I. Diffusion constants (units 10^{-8} cm^2 s^{-1}) obtained from the best fits with $Q = 0.06$ (shown by the solid lines in Figs. 2 and 3). The values in parentheses correspond to $Q = 0$.

θ	$D(\xi = 0.8\ \mu m)$		$D(\xi = 0.4\ \mu m)$	
30°	4.68 ± 0.05	(4.46 ± 0.06)	4.44 ± 0.12	(4.22 ± 0.13)
50°	4.66 ± 0.07	(4.46 ± 0.09)	4.41 ± 0.11	(4.21 ± 0.12)
70°	4.71 ± 0.06	(4.51 ± 0.07)	...	
90°	4.81 ± 0.07	(4.55 ± 0.08)	4.76 ± 0.02	(4.54 ± 0.02)[a]
110°	4.94 ± 0.05	(4.68 ± 0.07)	...	

[a]Bulk value.

vicinity of a reflecting wall may strongly differ from the bulk function as a result of the combined effect of the wall's reflection and the finite scattering volume in the evanescent-wave geometry. This introduces a long tail ($t^{-1/2}$) behavior in the longitudinal part of the correlation spectrum, but will be detected only if the transverse correlation function decays on a larger time scale. If the wall merely acts as a mirror, as we have assumed in our experiment, the changes in the spectrum become negligible for $\theta \geq 90°$. However, if surface-fluid interactions result in a slowing down of the transverse diffusion (critical surface transition,[3] for example), the changes in the longitudinal component will play an important role at all angles. Furthermore, we expect the $t^{-1/2}$ behavior of the correlation function to be enhanced by the wall-drag effect. Very close to the wall (z on the order of R, the particle's radius), the diffusion constant goes to zero linearly with z.[20] This creates a "trapping" layer which, in a similar way as the illuminated layer of thickness ξ, brings into the correlation function a $t^{-1/2}$ behavior characteristic of the probability for a given particle to be at a given time t in a finite layer of the suspension. The relative importance of this additional effect is on order of R/ξ, and it has been neglected in our presentation. However, in a more general way, we expect important changes in the correlation function when the longitudinal length scale of the problem (particle's radius, wall-suspension interaction range, etc.) becomes on the order of the optical penetration length ξ. This type of study is currently being done[17] with Brownian particles of radius $R \sim \xi$; it may be quite relevant for studying surface-transition dynamics, which can be viewed as the diffusion of a self-similar distribution of droplets.[21]

The authors wish to thank D. B. Ostrowsky for introducing them to evanescent-wave techniques, and for careful reading of the manuscript. Laboratoire de Physique de la Matière Condensée is Unité Associé No. 190, Centre National de la Recherche Scientifique.

[a]On leave from the University of Zhejiang, Zhejiang, China.

[1]N. J. Harrick, *Internal Reflection Spectroscopy* (Wiley, New York, 1967).

[2]*Photon Correlation and Light Beating Spectroscopy,* edited by H. Z. Cummins and E. R. Pike (Plenum, New York, 1974).

[3]K. Binder, in *Phase Transition and Critical Phenomena,* edited by C. Domb and J. L. Lebowitz (Academic, New York, 1983), Vol. 8.

[4]C. Allain, D. Ausserre, and F. Rondelez, Phys. Rev. Lett. **49**, 1694 (1982).

[5]N. L. Thompson, T. P. Burghardt, and D. Axelrod, Biophys. J. **33**, 435 (1981).

[6]D. Axelrod, N. L. Thompson, and T. P. Burghardt, J. Microsc. (Oxford) **129**, 19 (1983).

[7]D. Aussere, H. Hervet, and F. Rondelez, Phys. Rev. Lett. **54**, 1948 (1985).

[8]D. Beysens and S. Leibler, J. Phys. (Paris), Lett. **43**, L133 (1982).

[9]B. K. Lok, Y. L. Cheng, and C. R. Robertson, J. Colloid Interface Sci. **91**, 87 (1983).

[10]El-Hang Lee, R. E. Benner, J. B. Fenn, and R. K. Chang, Appl. Opt. **18**, 862 (1979).

[11]J. C. Selser, K. J. Rothschild, J. D. Swalen, and F. Rondelez, Phys. Rev. Lett. **48**, 1690 (1982).

[12]O. Bryngdahl, in *Progress in Optics,* edited by E. Wolf (North-Holland, New York, 1983), Vol. 11.

[13]D. B. Ostrowsky, A. M. Roy, and J. Sevin, Appl. Phys. Lett. **24**, 553 (1974).

[14]S. Chandrasekhar, Rev. Mod. Phys. **15**, 1 (1943).

[15]E. L. Elson and D. Magde, Biopolymers **13**, 1 (1974).

[16]D. Magde, E. L. Elson, and W. W. Webb, Biopolymers **13**, 29 (1974).

[17]K. H. Lan, N. Ostrowsky, and D. Sornette, to be published.

[18]*Handbook of Mathematical Functions,* edited by M. Abramowitz and I. A. Stegun (Dover, New York, 1968), p. 299.

[19]M. Hurd, *et al.,* in *Proceedings of the Fourth International Conference on Photon Correlation Techniques in Fluid Mechanics,* edited by W. T. Mayo, Jr., and A. E. Smart (Joint Institute of Aeronautic Acoustics, Stanford University, Palo Alto, CA, 1980).

[20]G. K. Batchelor, J. Fluid Mech. **74**, 1 (1976).

[21]M. E. Fisher and P. G. de Gennes, C.R. Acad. Sci., Ser. B **287**, 207 (1978).